Variations in triple isotope composition of dissolved oxygen and primary production in a subtropical reservoir

Hana Jurikova[1†], Tania Guha[1], Osamu Abe[2], Fuh-Kwo Shiah[1], Chung-Ho Wang[3], and Mao-Chang Liang[1,4,5]

[1]Research Center for Environmental Changes, Academia Sinica, 11529 Taipei, Taiwan
[2]Graduate School of Environmental Studies, Nagoya University, Chikusa, 464-8601 Nagoya, Japan
[3]Institute of Earth Sciences, Academia Sinica, 11529 Taipei, Taiwan
[4]Graduate Institute of Astronomy, National Central University, 32001 Jhongli, Taiwan
[5]Department of Physics, University of Houston, Houston, TX 77004, USA
[†]Now at: GEOMAR Helmholtz-Zentrum für Ozeanforschung Kiel, Wischhofstr. 1-3, 24148 Kiel, Germany

Correspondence to: Mao-Chang Liang (mcl@rcec.sinica.edu.tw)

Abstract. Lakes and reservoirs play an important role in the carbon cycle, and therefore, monitoring their metabolic rates is essential. The triple oxygen isotope anomaly of dissolved O_2 [$^{17}\Delta = \ln(1+\delta^{17}O) - 0.518 \times \ln(1+\delta^{18}O)$] offers a new, in situ, perspective on primary production, yet little is known on $^{17}\Delta$ from freshwater systems. We investigated the $^{17}\Delta$ together with oxygen-argon ratio ($\Delta O_2/Ar$) in the subtropical Feitsui Reservoir in Taiwan from June 2014 to July 2015. Here, we present the seasonal variations in $^{17}\Delta$, GP (gross production), NP (net production) and the NP/GP (net to gross ratio) in association with environmental parameters. The $^{17}\Delta$ varied with depth and season, with values ranging between 19 and 186 per meg. Low GP rates, typically below 200 mg C m^{-2} d^{-1} were observed in winter, while high GP rates, between 436 and 554 mg C m^{-2} d^{-1}, were recorded towards the end of the summer and in autumn. The NP was low and negative from October to February, however it dominated the overall metabolic balance of the reservoir implying the reservoir was net heterotrophic on annual basis. The estimated average annual GP was 160 g C m^{-2} $year^{-1}$ and NP was -50 g C m^{-2} $year^{-1}$. Comparisons between GP rates obtained from the isotope mass balance approach and ^{14}C bottle incubation method (^{14}C-GP) showed consistent values on the same order of magnitude with a GP/^{14}C-GP ratio of 0.6±0.3. Finally we noted that, although typhoon occurrences were scarce, higher than average $^{17}\Delta$ values and GP rates were recorded after typhoon events.

Key words. Triple oxygen isotope anomaly, ^{17}O-excess, oxygen-argon ratio, ^{14}C bottle incubations, carbon cycle, primary production, gross production, net production, freshwater system, Feitsui Reservoir

1 Introduction

It is well established that marine photosynthesis plays a critical role in the global biogeochemical cycling of carbon and oxygen that sustain the great majority of ecosystems on our planet. Recent studies show that freshwater systems constitute a significant component of these cycles and deserve closer attention (Cole et al. 2007, Tranvik et al. 2009, Valdespino-Castillo et al. 2013). Assessing primary production (PP) and providing accurate estimates of ecosystem metabolic rates is therefore a key for understanding each system's fluxes and variability in biogeochemical cycling.

Traditionally, PP has been evaluated by in vitro ^{14}C bottle incubation method introduced by Steeman-Nielsen (1952). However, these measurements are associated with a number of biases and the interpretation of the PP estimates is problematic. The main drawback is the in vitro methodology, which involves the removal of plankton communities from the natural environment and confining them into a small volume of water, with variability in PP observed under laboratory conditions. Because the distribution of plankton is heterogeneous in time and space, these experiments can only provide local and instantaneous PP rates, which do not reflect the time-averaged mean PP. The PP rates observed in vitro therefore can not be fully representative of natural PP rates (e.g. Harrison and Harris 1986, Marra 2002).

Over a decade and half ago, Luz et al. (1999) and Luz and Barkan (2000) introduced the triple oxygen-isotopes technique or the ^{17}O-excess ($^{17}\Delta$), which allows to assess PP in situ. The excess is defined as

$$^{17}\Delta = ln(1 + \delta^{17}O) - \lambda \times ln(1 + \delta^{18}O) \tag{1}$$

where the isotopic compositions $\delta^{17}O$ and $\delta^{18}O$ represent the deviation of the abundance ratio of an isotopic and normal species in a sample relative to that of a standard: $\delta^{*}O = ([^{*}O]/[^{16}O])_{sample}/([^{*}O]/[^{16}O])_{standard}-1]$, $^{*}O$ is either ^{17}O or ^{18}O. Here, $\delta^{17}O$ and $\delta^{18}O$ are expressed with respect to atmospheric air O_2. Following Luz and Barkan (2005), the factor λ is taken to be 0.518. The basic premise of this method lies in the processes fractionating O_2 isotopologues. While photochemical reactions in the stratosphere (the coupled chemistry between O_2, O_3, and CO_2) give rise to a non-mass-dependent signal in the atmospheric O_2 (Luz et al. 1999), respiration and photosynthesis fractionate O_2 in a mass-dependent way (the ^{17}O enrichment is approximately half of the ^{18}O relative to ^{16}O), which in a marine or aquatic systems allows for distinguishing the O_2 produced biologically from air O_2 entraining during gas exchange. Respiration modifies the dissolved O_2 concentrations in water but does not affect the $^{17}\Delta$, because the relative proportions of $\delta^{17}O$ and $\delta^{18}O$ remain the same. The respiratory effect on dissolved O_2 saturation can be evaluated using oxygen/argon ratios, considering the biological oxygen supersaturation expressed as $\Delta O_2/Ar$ (defined below in Eq. 4). This is because O_2 and Ar have similar physical properties, but the latter does not have biological sources or sinks. Although the PP evaluation based on the co-variation of both the $\delta^{17}O$ and the $\delta^{18}O$

values provides a more accurate assessment (Prokopenko et al. 2011, Kaiser 2011), the concept of $^{17}\Delta$ remains a valuable tool for tracing biologically produced O_2 and resolving the associated dynamics in the ocean. Up-to-date this joint geochemical budget approach ($^{17}\Delta$ or $\delta^{17}O$ and $\delta^{18}O$, together with $\Delta O_2/Ar$) has been applied widely to study marine production in the Atlantic (Luz and Barkan 2009, Quay et al. 2012), Pacific (Hendricks et al. 2005, Sarma et al. 2005, 2006,

5   2008, Quay et al. 2010, Prokopenko et al. 2011, Stanley et al. 2010, Juranek et al 2010, 2012, Munro et al. 2013) and the Southern Ocean (Reuer et al. 2007, Hamme et al. 2012, Huang et al. 2012, Castro-Morales et al. 2013), yet other oceanic basins and freshwater systems in general, with the exception of a case study in Lake Kinneret (Luz and Barkan 2000) remain by far and largely unstudied.

10   In this study, we extend the applicability of the $^{17}\Delta$ method in an aquatic system. We use the $^{17}\Delta$ method to trace the photosynthetic O_2 fate and to investigate the seasonal changes in PP in a semi-closed subtropical reservoir in Taiwan over the period of one year. We demonstrate that this approach offers new perspectives on PP in lakes. In an effort to contribute to the understanding of production rates measured in situ using the $^{17}\Delta$ method and the in vitro estimates from the ^{14}C bottle incubation approach, and to expand this to freshwater systems, we provide thorough comparisons between the respective

15   rates. In addition, we show data on the isotopic composition ($\delta^{18}O$, δD, and $^{17}\Delta$) of water from the reservoir. Understanding the isotopic composition of the Feitsui Reservoir water is crucial for accurate assessments of production rates using the $^{17}\Delta$ method and also offers insights into the biogeochemical/hydrological cycling of the reservoir. Ultimately, this paper presents a contribution to the studies on Feitsui Resevoir, a socio-economically and ecologically important reservoir.

2 Methods

20   **2.1 Site description**

The subtropical Feitsui Reservoir, located in northern Taiwan, is the country's second largest reservoir by volume (first is Tsengwen Dam in the south), serving as the main water source for over five millions of people in the Taipei metropolitan area. The domestic demand is supplied by water releases from the Feitsui Reservoir and unregulated flow from Nanshin Creek downstream of the watershed. The upstream watershed encompasses the Beishi stream basin a branch of Xindian

25   River, one of the three major tributaries of Tamsui River. The total catchment area of the reservoir is 303 km^2 and storage volume at normal maximum water level is 406 million m^3. The mean depth of the watershed is 40 m with maximum depth of 113 m near the dam site. The mean daily inflow to Feitsui Reservoir is ~30 m^3/s and the amount of water released depends on the reservoir's storage capacity and whether flow from Nanshin Creek is sufficient to supply domestic demand (Shiau and Wu 2010). In the past the reservoir was found to alternate between mesotrophic and oligotrophic states (Kuo et al. 2003)

30   although more recent studies (Kuo et al. 2006) observed a trend towards eutrophication. In 2012 according to Carlson's

3

Trophic State Index (CTSI) the reservoir was in a mesotrophic state. In order to prevent deterioration of water quality, the watershed is protected by the Feitsui Reservoir Administration with restricted access to the water as well as adjacent areas and any commercial and recreational activities are prohibited. In addition, since January 1988 the Feitsui Reservoir Administration operates a meteorological station that provided direct wind speed measurements 10 m above the water level and rainfall data used in this study. Typhoon information was obtained from a typhoon database (http://rdc28.cwb.gov.tw/TDB/ctrl_typhoon_range_search).

2.2 Physical structure and mixing in the water column of Feitsui Reservoir

Current assessments of PP rates rely on steady-state assumption. Whether the approximation is valid requires careful assessment and can be verified by studying the physical structure of the water body. Feitsui Reservoir is a typical monomictic system (characteristic of subtropical lakes), that stays thermally stratified throughout the greater part of the year, with changing intensity of winter vertical mixing depending on the meteorological conditions. The topographic characteristics of the reservoir, a large water mass located in a valley make its physical structure (i.e., water temperature) fairly simple and stable over the seasonal scale (Itoh et al. 2015). The residence time of water in the reservoir tends to be rather long; throughout our study we estimated it to be about 150 days, comparable to durations reported in the past (150 days reported by Kuo et al. 2003 and 115 days reported by Chen et al. 2006), sufficiently long to mix horizontally well. Field measurements as well as model simulation by Kuo et al. (2003) reported alike trends in dissolved oxygen concentration throughout a period of 12 months, recorded at the Dam Site (S1) and at the Wu-Tan station situated on the other side of the reservoir upstream of the Beishi Creek. A comparison between the top, middle, and bottom layers of the water column showed that the reservoir is horizontally rather uniform and is not affected significantly by horizontal water advection (Kuo et al. 2003).

2.3 Water sampling and sample preparation

Sampling was carried out at station S1 (24.9 E, 121.566667 N, Fig. 1) in the Feitsui Reservoir in the upper 100 m, located in the deepest region of the lake (~113 m). Water samples were collected using 5-L GO-FLO samplers with a manual messenger. For dissolved oxygen analysis, we collected waters at 9 depths (1, 5, 10, 15, 20, 30, 50, 70 and 90 m) during 13 separate trips to the reservoir, covering one full year from June 2014 to July 2015. Sampling for isotope analysis of water started later in September 2014.

Vertical profiles of temperature, chlorophyll *a,* and dissolved oxygen concentration were recorded routinely using Ocean Seven 316 CTD (IDRONAUT, Italy) multiparameter probe. A PAR sensor (BioTech) was used to measure photic irradiance. The casts were typically carried out on weekly basis during the summer and every two weeks during the winter. The

4

accuracy of dissolved oxygen measurements was verified against in vitro measurements; water samples collected from 10 depths (0, 2, 5, 10, 15, 20, 30, 50, 70 and 90 m) were siphoned intro triplicate 60 ml bottles (Wheaton) and a colorimetric method of Pai et al. (1993) was adopted for in vitro dissolved O_2 determination with precision of 0.2 % r.s.d. (full scale). We used a conservative approach for determining the mixed layer depth based on visual inspections of vertical temperature and dissolved oxygen profiles, to ensure the well-mixed layer only is described, without influences from the thermocline. For visualization and analysis of the profile data, we used Ocean Data View (ODV, Schlitzer 2015).

Dissolved gasses were extracted from water following Emerson et al. (1995) and Luz et al. (2002). In summary, 300 ml flasks with LouwersHapert© O-ring stopcock, containing 50 µl of saturated $HgCl_2$ solution, were evacuated prior to sampling and closed with a water lock. Approximately 150 ml of water sample was collected in the flask, leaving 150 ml of headspace for gases to exsolve. Once stopcock closed, the port was filled with the same water as sampled and sealed with a rubber cap to avoid air contamination. All samples were equilibrated for 24 h in a shaker at room temperature. After equilibration, water was removed from the samples and the flasks were subsequently connected to a preparation system for removal of water vapour, CO_2, and other condensable molecules at liquid nitrogen temperature. The extracted gases were then either stored in a sealed glass tube or directly introduced to a GC system (Thermo Scientific TRACE Gas Chromatograph) for complete removal of N_2 after which only O_2 and Ar remained the main components in the gas mixture. The separation was done using a chromatographic column (3 m long, 1/8" SS tube, packed with molecular sieve 5A at mesh 60/100), modified from Barkan and Luz (2003). During the separation the chromatographic column was kept at room temperature, and the yielded oxygen-argon mixture was absorbed onto two pellets of molecular sieve (1.6 mm, 5A, manufactured by SUPELCO) for subsequent isotopic analysis, following Abe (2009) with slight modifications.

2.4 ^{14}C bottle incubations

In summary, water samples were incubated for approximately 2~3 hours. A chlorophyll-normalized photosynthesis rate versus light intensity below the onset of photoinhibition (i.e. P^B-I) model, proposed by Jassby and Platt (1976) was used to calculate primary production over 24 hours performed using an artificial light source to mimic the solar spectrum at an intensity controlled according to the solar irradiance measured in situ. The ^{14}C rates reflect gross C production and are integrated for the entire euphotic zone. Detailed description of methodology for ^{14}C incubation experiments is provided in Shiah et al. (1996).

2.5 Stable isotope analysis of dissolved oxygen

$\delta^{17}O$ and $\delta^{18}O$ in O_2 from the purified oxygen-argon mixture (as explained in Sec. 2.2) were determined by dual inlet mass spectrometry (Thermo Scientific Finnigan MAT 253 Stable Isotope Ratio Mass Spectrometer). Each sample was run for 3

acquisitions, 12 changeover cycles each, thus the reported δ-values present the average of 36 cycles. The analytical errors (1-σ standard error of the mean n=36 multiplied by Student's t-factor for a 95 % confidence limits, reported following Barkan and Luz (2003)) for $\delta^{17}O$ and $\delta^{18}O$ were 0.013 ‰ and 0.006 ‰, respectively. Our actual and long-term precision (1-σ standard deviation) established from routine measurements (n = 36) of atmospheric O_2 for $\delta^{17}O$, $\delta^{18}O$, and $^{17}\Delta$ was 0.017 ‰, 0.030 ‰, and 6 per meg, respectively.

The O_2/Ar ratio was obtained by peak jumping; a sequential measurement of m/z '32' and '40' in the same collector (with the idle and integration times 20 and 4 s, respectively, following Barkan and Luz 2003) prior to isotopic ratio analysis. The O_2/Ar ratio is expressed in the standard δ-notations and calculated as $\delta O_2/Ar$ (‰) = $[(32/40)_{sample}/(32/40)_{standard}-1]10^3$. The long-term precision (1-σ standard deviation) of routine measurements of atmospheric air was better than 5 ‰. For all water samples the final $\delta O_2/Ar$ values were corrected for the distribution of gases between the headspace and water in the sampling flasks, following Luz et al. (2002) and normalized to air. To verify the purity of the collected oxygen-argon mixture after the GC separation, we have also included regular monitoring of m/z '28' signal during peak jumping. We did not detect any significant presence of N_2 during the course of the study, either in atmospheric air or water samples for dissolved oxygen analysis. For all analysed samples the N_2/O_2 signal ratio was lower than 0.001.

Similar to Luz and Barkan (2003) and Abe and Yoshida (2003), we found that the values of $\delta^{17}O$, $\delta^{18}O$ and $^{17}\Delta$ are affected by the O_2/Ar ratio, presumably due to interference with the ion source of the mass spectrometer. Although this effect on the $\delta^{17}O$ and the $\delta^{18}O$ values is minor, it may significantly affect the $^{17}\Delta$. We have calculated the dependencies of the $\delta^{17}O$, $\delta^{18}O$ and $^{17}\Delta$ on the O_2/Ar ratio, derived from measurements of aliquots of pure O_2 with added different amounts of Ar and applied the correction to the reported final isotopic values. The regression slopes for $\delta^{17}O$, $\delta^{18}O$ and $^{17}\Delta$ were 0.00001 ‰/‰ ($R^2 = 0.66$), -0.00002 ‰/‰ ($R^2 = 0.79$), and 0.0217 per meg/‰ ($R^2 = 0.99$), respectively.

To minimize the influence of Ar and for obtaining more precise results, we used a working O_2-Ar reference mixture from pure gases (>99.999 %) with the proportion of O_2/Ar ~20:1, similar to the O_2-Ar solubility ratio in surface water (Benson and Krause 1984, Krause and Benson 1989, Barkan and Luz 2003). The integrity of the standard was checked regularly by measuring aliquots of atmospheric O_2. For every set of water samples from Feitsui Reservoir (one set representing one trip to the reservoir) three aliquots of atmospheric O_2 were prepared and measured against the same aliquot of working reference gas mixture as used for the water sample set.

To evaluate the reproducibility and performance of sample preparation, we prepared air-equilibrated water. The equilibration was achieved by continuous stirring of 8 L of deionised water with added $HgCl_2$ in a circulator with temperature control at

25 °C over a period of 72 hours. Dissolved gases were extracted following the same procedure as applied for the reservoir samples (see Sec. 2.2). The reproducibility (1-σ standard deviation) for the analysis of equilibrated water samples (n = 3) was 0.020 ‰, 0.037 ‰, and 3 per meg for $\delta^{17}O$, $\delta^{18}O$, and $^{17}\Delta$, respectively and 4.6 ‰ for $\delta O_2/Ar$ (Table 1).

2.6 Stable isotope analysis of water

To identify the source of water in the reservoir, we carried out additional analyses of δD and $\delta^{18}O$ in the H_2O molecule of reservoir water. For this, water samples were collected in 15 ml centrifuged vials and sealed with Parafilm M® to prevent any isotopic alteration due to evaporation. Prior to analysis, water was transferred to 2 ml vials with the aid of a pipette and analysed in a Picarro L2130-I Isotopic H_2O Analyser, following Laskar et al. (2014). δD and $\delta^{18}O$ values are expressed with respect to VSMOW (‰). The $^{17}\Delta$ for 2014 water samples was determined using CoF_3 fluorination method following Barkan and Luz (2005). Briefly, an aliquot of 5 μl of water was converted to O_2 by injecting it to a CoF_3 containing reaction tube heated at 370 °C under helium flow. The evolved oxygen gas was collected in a 13X molecular sieve U-trap at liquid nitrogen temperature, and then determined by dual-inlet mass spectrometry (Thermo Scientific Delta Plus). Each sample was run for 80 changeover valve cycles, i.e., 80 sample-standard combinations. Mean standard deviations (1-σ) of multiple duplicate analyses for various waters (including VSMOW2, GISP, and SLAP) for $\delta^{17}O$, $\delta^{18}O$, and $^{17}\Delta$, were 0.086 ‰, 0.168 ‰, and 11 per meg, respectively. For 2015 samples, we used water-CO_2 equilibration method (with water-CO_2 ratio about 100:1 mole/mole) to determine the $^{17}\Delta$ value of the equilibrated CO_2 (Mahata et al. 2013, 2016) first and then to that of water, calibrated against three aforementioned international standards. The averaged reproducibility for $\delta^{18}O$ and $^{17}\Delta$ were 0.05‰ and 15 per meg, respectively.

2.7 Gross and net production calculations

Aquatic primary production (PP), the synthesis of organic compounds from aqueous carbon-containing species, in a steady state system may be distinguished as gross production (GP) and net production (NP). The GP represents the total carbon fixed by primary producers, and the NP represents the carbon available to the heterotrophic community. The NP is therefore the difference between GP and community respiration and corresponds to the overall metabolic balance of an ecosystem. NP can be positive or negative. NP is positive when GP exceeds respiration and the ecosystem may export or store organic C. The value is negative when respiration exceeds GP and the ecosystem respires more organic C than was able to produce. Both GP and NP are terms of fundamental interest in carbon cycle studies.

To quantify gross production rates from $^{17}\Delta$ values, a simple box model may be applied; mixed layer gross oxygen production (GOP) is assumed at steady state with respect to $^{17}\Delta$ and O_2 concentrations, and vertical mixing is neglected, following Luz and Barkan (2000).

$$GOP = K\,C_o\,(^{17}\Delta - {}^{17}\Delta_{eq})/({}^{17}\Delta_{bio} - {}^{17}\Delta) \tag{2}$$

where C_o is the O_2 concentration at saturation using solubility coefficients from Benson and Krause (1984) and K is piston velocity (the coefficient for gas-exchange; Crusius et al. 2003, Wanninkhof et al. 2009). Here the $^{17}\Delta_{eq}$ is the air-water equilibrium, deviating from zero due to isotopic fractionation during O_2 invasion and the $^{17}\Delta_{bio}$ represents the value of purely biologically produced O_2. We calculated K (the piston velocity) from daily wind speeds at Feitsui Reservoir according to Wanninkhof et al. (1987) and Vachon and Prairie (2013), based on studies of gas transfer velocities in lakes of comparable sizes to Feitsui Reservoir. Because the gas concentrations in the mixed layer depend on the recent history of wind speeds, we averaged K over the residence time of O_2 in the mixed layer preceding sampling, based on the mixed layer depth and gas transfer coefficient.

Eq. 2 however represents a mathematical approximation, to provide a first order realization of processes and sources that affect the GP. This simplified formulation may introduce large errors, in particular in ecosystems with elevated export ratios. Prokopenko et al. (2011) and Kaiser (2011) derived an improved 'dual-delta approach', which we applied for estimating GP rates in the Feitsui Reservoir, where the GOP may be directly calculated from the measured $\delta^{17}O$ and $\delta^{18}O$ values, as follows:

$$GOP = K C_o \frac{\left(1 - \frac{10^{-3}\delta^{17}O_{eq}+1}{10^{-3}\delta^{17}O+1}\right) - \left(1 - \frac{10^{-3}\delta^{18}O_{eq}+1}{10^{-3}\delta^{18}O+1}\right)}{\left(\frac{10^{-3}\delta^{17}O_p+1}{10^{-3}\delta^{17}O+1} - 1\right) - \left(\frac{10^{-3}\delta^{18}O_p+1}{10^{-3}\delta^{18}O+1} - 1\right)} \tag{3}$$

where δ^*O is the measured value in a sample, δ^*O_{eq} is the air-water equilibrium, and δ^*O_p represents the photosynthetic O_2.

To estimate the net oxygen production (NOP) rates, we have used the O_2/Ar measurements, following the biological O_2 supersaturation concept for net photosynthetic production. Because the physical properties of O_2 and Ar are similar, and Ar has no biological sources and sinks, measurements of Ar concentration in water may be used to remove physical contributions to O_2 supersaturation. The biological oxygen supersaturation $\Delta O_2/Ar$ is defined as the relative deviation of the O_2/Ar in a sample to the O_2/Ar at equilibrium with the atmosphere (Craig and Hayward 1987, Spitzer and Jenkins 1989, Emertson et al. 1995, Kaiser et al. 2005) and may be calculated as follows:

$$\Delta O_2/Ar = \frac{(\delta O_2/Ar)}{(\delta O_2/Ar)_{eq}} - 1 \tag{4}$$

Assuming the mixed layer is at steady state, NOP can be calculated following Luz et al. (2002):

$$NOP = K \, C_o \, \Delta O_2/Ar \qquad\qquad (5)$$

A shortcoming associated with the calculation of PP rates from dissolved O_2 isotopes is that the rates are in O_2 units, instead of C based units, and the conversion between them is not straightforward. To convert between O_2 and C based rates, we follow the common approach presented earlier (e.g., Hendricks et al. 2014, Juranek et al. 2012). GOP from $^{17}\Delta$ is greater than gross C production because it measures total oxygen produced regardless of its fate, such as the fraction of O_2 produced which is linked to Mehler reaction and photorespiration. To scale GOP to gross C production, we account for this fraction following Laws et al. (2000) and apply a photosynthetic quotient (PQ) of 1.2. We convert NOP to a comparable C flux using a PQ of 1.4, for new production (Laws 1991).

3 Results

3.1 Hydrography

We refer to our monthly sampling dates as MMMYY for convenience. The subtropical Feitsui Reservoir was thermally stratified for the great part of the year, with a distinct seasonal thermocline (Fig. 2a). In spring seasonal stratification developed (APR15), and the lake remained well stratified with a shallow epilimnion with temperature above ~30 °C throughout the warmer months in the top 10 m layer. In summer, the reservoir was strongly stratified as the result of continued heating of the surface water and the mixed layer remained shallow, typically about 3 – 5 m deep, as observed in JUN14, AUG14, APR15, MAY15 and JUL15. Although the thermal structure of the reservoir controls the gas exchange during the warm months, processes such as rainfall and windstorms may entrain atmospheric air to the thermocline, as showed from dissolved O_2 and $\Delta O_2/Ar$ vertical profiles (Fig. 2c and 4c), playing a critical role in influencing the conditions in the mixed layer. From SEP14 and OCT14, as a result of decreasing ambient temperature and gradual cooling of surface water the mixed layer deepened reaching 11 and 23 m, respectively. In DEC14 the thermal stratification became weaker initiating the winter overturn, resulting in well-mixed epilimnion of ~22 °C to 34 m depth, and a decreasing temperature gradient in the metalimnion. In JAN15 the mixed layer was deepest at 51 m. The mixed layer remained deep throughout FEB15 (40 m) when the reservoir was coolest and nearly homothermal in FEB15 of ~17 °C in the epilimnion and ~16°C in the hypolimnion.

The Chlorophyll *a* (Chl *a*) fluorescence (Fig. 2b) in the reservoir was predominantly restricted to the epilimnion and the upper thermocline. The distribution and concentration varied with seasons and with the occurrence of stochastic events (such as storms, strong rainfall or typhoons) that enhanced the photosynthetic activity in the phytoplankton. Chl *a* concentration was high from JUN14 to SEP14, with a subsurface maximum below the mixed layer at ~10 m, averaging to 15 mg m^{-3} and occasionally above 20 mg m^{-3}. In late SEP14, the Chl *a* maximum shifted to the surface. No apparent maximum was observed in OCT14 when Chl *a* concentration was rather uniform throughout the mixed layer of average ~8 mg m^{-3} in the upper 23 m. From DEC14 to FEB15, Chl *a* concentration remained low at ~3 mg m^{-3}, with the exception of a small episodic subsurface maximum of ~5 mg m^{-3} at 8 m in JAN15. In spring, Chl *a* concentration started to increase at the surface averaging ~5 mg m^{-3}, followed by later appearance of a subsurface maximum at 12 m of ~8 mg m^{-3}. A short episodic decrease in Chl *a* was recorded in APR15, a likely result of cooler ambient temperature than normal and frequent precipitation. In MAY15, Chl *a* concentration increased again and high subsurface maximum of >10 mg m^{-3} formed at 15 m.

The dissolved oxygen (DO) concentration and saturation levels (Fig. 2c) varied in association with O_2-Ar ratios measured, indicating the availability of dissolved O_2 supplied by primary production, aeration or mixing processes. The epilimnion remained saturated throughout the year, in the thermocline DO varied greatly; DO was undersaturated from AUG14 to DEC14 (<50 %), reached near-saturation levels during the winter and from APR15 to JUN15 remained supersaturated (>100 %). In spring and summer the DO reached the hypolimnion where the saturation was typically above 50%. Conversely, from early AUG14, throughout autumn and winter the hypolimnion was undersaturated (below 50 %) with minimal DO content.

3.2 Isotopic composition of water

In addition to dissolved O_2, we have measured the isotopic composition of water in the Feitsui Reservoir throughout the different seasons. The isotopic composition of water varied in both $\delta^{18}O$ (Fig. 3a) and δD (Fig. 3b) seasonally and vertically. Overall, the variation of $\delta^{18}O$ was smaller than that of δD, varying between -6.5 and -5.3 ‰ in $\delta^{18}O$ and between -37.1 and -25.4 ‰ in δD. The general pattern for both, δD and $\delta^{18}O$, showed more depleted values during autumn, followed by gradual enrichment throughout the winter, spring and early summer. No statistically significant (within errors) seasonal variation was found between $^{17}\Delta$ values obtained by the fluorination method and by water-CO_2 equilibration. We therefore averaged the $^{17}\Delta$ over the year, with the resultant $^{17}\Delta$ of 222±9 per meg, representing the $^{17}\Delta$ of water in the Feitsui Reservoir. The insignificance in $^{17}\Delta$ seasonality is consistent with the small overall variation in $\delta^{18}O$ and also with the long residence of water in the reservoir.

3.3 The $^{17}\Delta$ of dissolved O_2

10

The $^{17}\Delta$ signal of dissolved O_2 varied with depth and seasons (Fig. 4b). The overall range of the $^{17}\Delta$ values measured ranged between the maximum of 186 per meg in late AUG14 and JUL15 and minimum of 19 per meg in JUN14. The annual mean $^{17}\Delta$ at the surface (1 m) was 59±13 per meg and remained constant throughout the year, with the exception of late SEP14 and JUL15, when the surface values were higher, recording 91 and 71 per meg, respectively and coinciding with an episodic shift of Chl a maximum towards the surface (Fig. 2b). During months with persistent thermal stratification in the reservoir, the $^{17}\Delta$ followed a similar vertical pattern, with distinct $^{17}\Delta$ values. From JUN14 to early SEP14, when the mixed layer was very shallow (~3-5 m), the $^{17}\Delta$ signal accumulated below, in the upper thermocline, with a peak exceeding 150 per meg observed typically at ~10-20 m depth. Below the thermocline at ~50 m depth in AUG14 and SEP14 the $^{17}\Delta$ was low showing signals characteristic of surface water. In late SEP14 and OCT14 as the mixed layer deepened gradually, we observed a corresponding trend for the $^{17}\Delta$, with the peak in the signal deepening (182 and 137 per meg at ~20 and 30 m, respectively) following the mixed layer boundary. In DEC14 the deep mixed layer and decreasing importance of the thermal stratification facilitated increased gas exchange throughout the water column resulting in low and rather uniform $^{17}\Delta$ values in the water column of 55±5 per meg. This trend continued throughout the winter period, during which the $^{17}\Delta$ values stayed comparatively low and less variable. The onset of thermal stratification during the spring allowed for $^{17}\Delta$ to increase below the mixed layer; in APR15 we observed a developing peak in the $^{17}\Delta$ signal of 99 per meg at 10 m. The $^{17}\Delta$ increased throughout MAY15, and in JUN15 and JUL15 the accumulated $^{17}\Delta$ signal was high at 10-30 m, averaging 157±35 per meg, coinciding with the observed DO supersaturation (Fig. 2c) and high $\Delta O_2/Ar$ (Fig. 4c). Converse to the trend from JUL14, in JUL15 the $^{17}\Delta$ signal was high below the mixed layer and throughout the whole water column. Although samples from regions below 50 m and 70 m were limited due to insufficient amount of gas for isotope analysis, overall the $^{17}\Delta$ values tend to increase towards the bottom of the hypolimnion, in particular high $^{17}\Delta$ was measured at 70 m in late AUG14, SEP14, and JUL15 of 133, 131 and 165 per meg, respectively.

3.4 Gross and net production

Following Prokopenko et al. (2011) and Kaiser (2011), we estimated PP rates in the Feitsui Reservoir from JUN14 to JUL15. The GP rates, NP rates and the NP/GP ratio obtained by the dual-delta approach are summarised in Table 2. Overall, the GP rates varied between 79 and 1195 mg C m^{-2} d^{-1}. The general pattern showed lower values during the winter months, 207, 121 and 79 for mg C m^{-2} d^{-1} for DEC14, JAN15 and FEB15, respectively, which may be considered as maximum production because the mixed layer is deeper than the euphotic zone in winter. A slight increase in the GP was observed in JUN14, APR15, MAY15 and JUN15 varying between 247 and 348 mg C m^{-2} d^{-1}. Throughout AUG14 and in early SEP14 and in OCT14, production was high varying between 436 and 554 mg C m^{-2} d^{-1}. This represents the minimum GP for this period, because the mixed layer is shallower than the euphotic zone and therefore some production also took place below the mixed

layer, which may not be evaluated by the present model. Production was highest in late SEP14 and in JUL15, 912 and 1195 mg C m^{-2} d^{-1}, coinciding with typhoon events affecting the area of the Feitsui Reservoir.

Overall, the NP ranged between -4556 and 3491 mg C m^{-2} d^{-1}. The NP was negative from OCT14 to FEB15, varying between -2008 and -4556 mg C m^{-2} d^{-1}, indicating the reservoir was net heterotrophic in the mixed layer during the cooler months. Positive but lower NP rates were recorded in APR15, yielding 360 mg C m^{-2} d^{-1}. Throughout the rest of the year NP varied between 524 and 1347 mg C m^{-2} d^{-1}, implying the reservoir remained net autotrophic during the greater part of the year. Highest NP rates were observed in JUL15 measuring 3491 mg C m^{-2} d^{-1},

Using the GP and NP rates measured in our study, we estimated the annual C production in the Feitsui Reservoir. Excluding the measurements obtained during episodic typhoons (late SEP14 and JUL15), the average annual GP amounted to 119 g C m^{-2} $year^{-1}$ and the average annual NP was -165 g C m^{-2} $year^{-1}$. Taking into consideration typhoon events, the average annual GP increased to 160 g C m^{-2} $year^{-1}$, while the average annual NP decreased to -50 g C m^{-2} $year^{-1}$. For comparison, a model study by Lewis (2011) estimates the global average annual production per unit area for a lake 200 g C m^{-2} $year^{-1}$ for GP and 160 g C m^{-2} $year^{-1}$ for NP. While our GP estimates agree well with this projection, in particularly when the production rates take into account typhoon events, our NP rates lie at the lower end of the global average. The measured NP rates in the Feitsui Reservoir thus indicate that over the year the respiration exceeds gross primary production in the reservoir, affecting the net balances of carbon. Episodic events such as typhoon events seem to play a key role in the metabolism of Feitsui reservoir, and it is plausible that during years with frequent typhoon events the annual balance of the reservoir may shift to net autotrophy. Although some carbon storage is expected in the form of accumulation of organic matter to the sediments (Dean and Gorham 1988), our results indicate that from 2014 to 2015 Feitsui reservoir acted as a positive carbon source to the atmosphere.

4 Discussion

4.1 The $^{17}\Delta$ and $\Delta O_2/Ar$ tracers for photosynthesis and respiration

The schematics of $^{17}\Delta$ transport and variation are summarised in Fig. 5. The near-surface $^{17}\Delta$ value represents a balance between O_2 produced photosynthetically, which tends to increase the $^{17}\Delta$, and that from gaseous exchange with atmospheric O_2, which reduces the $^{17}\Delta$ value. The nearly constant surface $^{17}\Delta$ values measured in the Feitsui Reservoir throughout the year (59±13 per meg) suggest that the balance of these processes does not typically vary with seasons. In late SEP14 and in JUL15, the surface $^{17}\Delta$ values were 33 and 13 per meg higher, respectively, than the annual mean, indicating additional input from photosynthesis. Further analysis showed that in both cases, the samples were taken within a few days after typhoon

12

occurrences. Thus the resulting elevated $^{17}\Delta$ is likely to be a consequence of nutrient enrichment caused by typhoons, mediating enhanced vertical mixing and hence photosynthesis (see Sect. 4.5 for further details). Previous studies showed that in the Feitsui Reservoir phosphate plays a key role as the limiting nutrient, restricting the microbial production. The key processes that determine its availability are vertical mixing from changes in the mixed layer depth in the spring and typhoon intensity in summer and autumn (Tseng et al. 2010, Itoh et al. 2012). These processes therefore likely play a role in the distribution of the $^{17}\Delta$ signal in the water column as well as increase photosynthetic activity as a result of intensified production after nutrient enrichment.

High subsurface $^{17}\Delta$ may be primarily attributed to the decreasing importance of gas exchange with depth. This is particularly characteristic of the warmer months during which strong thermal stratification developed confining the primary producers to the thermocline (also showed by Chl *a*, Fig. 2b) where the conditions are optimal for phytoplankton growth, representing a compromise between light, temperature, and nutrient availability. From AUG14 to OCT14 we recorded high $^{17}\Delta$ (often above 150 per meg) values below the thermocline (5–30 m). It is likely that the local primary production was initially high, a possible result of a phytoplankton bloom influencing the observed $^{17}\Delta$ composition. Yet, the measured low $\Delta O_2/Ar$ values (about -1 to -3 %) and undersaturation of DO indicate O_2 consumption from AUG14 to OCT14 in the upper thermocline. In the absence of photosynthesis, the residual $^{17}\Delta$ signal thus points towards the lack of vertical mixing in the reservoir during this period as well as no influence from atmospheric air. At 50 m depth, we recorded $^{17}\Delta$ values, typical of near-surface water. Here, the $^{17}\Delta$ shows an inverse relationship to $\Delta O_2/Ar$ as well as DO, with lower $^{17}\Delta$ and higher $\Delta O_2/Ar$ and DO observed in AUG14 and SEP14 and increasing $^{17}\Delta$ and decreasing $\Delta O_2/Ar$ DO saturation observed in OCT14. Additionally, the signal also follows the thermal structure of the reservoir; from July to about November 2014 we observe well mixed epilimnion in the upper ~10 to 20 m and an extensive metalimnion to about 50–60 m, with strong thermal gradient before reaching hypolimnion below. It is likely that the low $^{17}\Delta$ origins from atmospheric air entrainment during early summer (June and July, DO profile, Fig. 2c).

Intrusion of surface water below the metalimnion has also been observed in previous studies and may also be supported by dust loading which results in an increase in total suspended material at depth (Tseng et al. 2010). Strong vertical mixing of air-saturated water down the water column in JUN15, indicated by the low $^{17}\Delta$ values, increased $\Delta O_2/Ar$, as well as DO, as a result of heavy rainfall (~ 700 mm accumulated precipitations during JUN14, comparing to ~340 and ~200 mm measured in JUL14 and AUG14, respectively, Fig. 6) may have supplied atmospheric O_2 to the metalimnion and the hypolimnion. As of early AUG14 at 50 m, the observed $^{17}\Delta$ signal possibly traces the remaining $^{17}\Delta$ signal from JUN15, locally confined due to the strong thermal gradient and unaltered by photosynthesis due to the lack of primary producers at this depth. The breaking down of both, the high $^{17}\Delta$ from ~20–30 m, and the low $^{17}\Delta$ from 50 m, throughout autumn is controlled by decreasing air

13

temperatures and the consequent weakening thermal stratification in the reservoir, also observed in other years (Itoh et al. 2012). Apart from storms and typhoons causing wind stress at the air-water interface or heavy precipitation, other processes that affect vertical mixing in the reservoir include instabilities caused by heat losses at the surface or as a result of lake processes such as seiches. Seiches were never evaluated in the Feitsui Reservoir, but they may play an important role in affecting the vertical transfer of the water masses, dissolved gases, and nutrients in the Feitsui Reservoir and should be considered in future studies.

Increase in the $^{17}\Delta$ towards the bottom of the lake (90 m samples) was observed during all seasons, originating likely from the transport of enhanced $^{17}\Delta$ values from the upper part of the water column and any photosyntheticallty induced changes to the signal before it reached the bottom. These samples however contained only small amounts of O_2 (saturation less than ~50 %), and therefore it is possible that minor photosynthetic contributions could significantly increase the $^{17}\Delta$ values, as result of vertical entrainment mentioned previously.

4.2 Uncertainties in PP rates

Although the improved dual-delta method presents a mathematically more accurate approximation than the previous $^{17}\Delta$ model, a number of uncertainties associated with both methods for estimating PP rates remain, and should be considered beforehand. Luz and Barkan (2000), Prokopeno et al. (2011), and Kaiser (2011) demonstrated that GP in the mixed layer could be determined from the measurements of $^{17}\Delta$ or the δ-values in dissolved O_2 using a steady state mixed layer oxygen budget model which allows for estimation of integrated gross productivity in the mixed layer over the residence time of mixed-layer O_2. It is important to note that this approach may underestimate GP on occasions when the euphotic zone is deeper than the mixed layer since the calculation accounts for GP in the mixed layer only. This may particularly affect PP estimates during summer months, when the photic layer is typically deeper than the mixed layer in subtropical reservoirs in general, and about 4 times deeper in the Feitsui reservoir. Furthermore, this model lacks terms for advection and vertical mixing. While the effect of these simplifications may be negligible in the open ocean (Emerson et al. 1997), lakes and reservoirs often feature a complex vertical and horizontal structure, the effect of which needs to be considered. Fortunately, given the rather simple physical structure of the Feitsui Reservoir horizontal inhomogenities may be neglected. The column inventory approach presented below (Sec. 4.3) provides a robust technique for assessing the contributions of vertical mixing and to estimate the production below the mixed layer.

The key parameter to constrain the GP and NP rates is the gas exchange rate between the mixed layer and the atmosphere. Presently this is best achieved by parameterization of wind speeds, which is commonly used in models with several empirical relationships between the wind speed and gas exchange rate (e.g. Clark et al. 1995, Ho et al. 2006, Wanninkhof et

14

al. 2009). Yet parameterization of wind speeds does not come without inaccuracies. While in most of the oceanic studies, the error associated with the parameterization is attributed to the accuracy of wind speed measurements and the relationship between the wind speed and gas exchange rate at very high or low wind speed conditions (Wanninkhof 1992). In freshwater systems, factors such as lake size and ecosystem heterogeneity present another important factor (Vachon and Prairie 2013) and should be taken into consideration when choosing an appropriate parameterization.

Apart from δ-values measured in samples, δ^*O_{eq} and δ^*O_p or $^{17}\Delta_{eq}$ and $^{17}\Delta_{bio}$ are important constituents of this method. δ^*O_{eq} or $^{17}\Delta_{eq}$ is rather well established and can be determined experimentally by air-water equilibrations, usually achieved by bubbling or stirring (Keedakkadan et al. 2015). The δ^*O_p or $^{17}\Delta_{bio}$ represents the photosynthetic O_2 composition, with controversy on these values discussed in the literature (e.g. Kaiser 2011, Luz and Barkan 2011, Nicholson 2011). The major problem lies in proper quantification of the value for $^{17}\Delta_{bio}$. Being closely dependent on the $^{17}\Delta$ of substrate water and less straightforward to measure, the $^{17}\Delta_{bio}$ value was previously often assumed to be the same as that of water. Recently, Luz and Barkan (2011) showed that a small difference exists between the substrate water values and the average composition of photosynthetic O_2 produced by phytoplankton. This potential bias has to be considered, in order to improve the accuracy of primary production estimates. Furthermore, whereas a uniform value for $^{17}\Delta$ of seawater may be applied to study PP in the ocean, $^{17}\Delta$ for a freshwater system of interest has to be determined because the isotopic composition of freshwater tends to vary geographically and among different water sources (Luz and Barkan 2010). For Feitsui Reservoir we determined 222 per meg for $^{17}\Delta$ of water, based on measurements of water samples collected throughout the year. The difference between the isotopic composition of Feitsui Reservoir water and that of photosynthetic O_2 provided by Luz and Barkan (2011), therefore reflects the associated fractionation between the substrate water and the photosynthetic O_2. To obtain the representative δ^*O_p and $^{17}\Delta_{bio}$ values for the Feitsui Reservoir, we consider these additional fractionations of 26 per meg and 3.306 ‰ for $^{17}\Delta_{bio}$ and $\delta^{18}O$, respectively, to our measured values of water and retrospectively calculate the $\delta^{17}O_P$.

Compared to the GP, estimating the net production is less complicated, since the model only requires the coefficient for gas exchange and a term describing the biological supersaturation. The second term can be constrained by the $\Delta O_2/Ar$ based on measurements from flask samples or determined in situ using a sensor for dissolved O_2 supersaturation, although the accuracy of the latter is inferior and may be less suitable for this purpose. Combining $^{17}\Delta$ and $\Delta O_2/Ar$ measurements we can get the net to gross production ratio (NP/GP), which is equivalent to an export ratio (Laws et al. 2000) describing the capacity of an ecosystem to export C. The NP/GP ratio can be far better constrained than the GP on its own, since it is independent of the gas exchange rate and the uncertainty in the ratio only depends on the error in the measurement of $^{17}\Delta$ and $\Delta O_2/Ar$.

15

4.3 Column inventory approach

As discussed previously (Sec. 4.1), in case of fast changing physical dynamics in a reservoir, a mixed layer budget by isotope mass balance calculation may not be applicable for the assessment of PP rates. To assess the relevance of this method for the Feitsui Reservoir, we tested an alternative mass balance model based on a whole column inventory approach (onwards referred to as column inventory approach). Unlike isotope mass balance limited to the mixed layer, the column inventory model requires time-series data of full profiles from the surface to the bottom of the lake, and is able to obtain the GP rates below the mixed layer, without steady-state assumptions.

Calculating the GP by the column inventory model is done by solving the following simultaneous equations:

$$^{16}O_t - {}^{16}O_{t-1} = {}^{16}P - {}^{16}C + {}^{16}I - {}^{16}E \tag{Eq. 5}$$

$$^{17}O_t - {}^{17}O_{t-1} = {}^{17}P - {}^{17}C + {}^{17}I - {}^{17}E \tag{Eq. 6}$$

$$^{18}O_t - {}^{18}O_{t-1} = {}^{18}P - {}^{18}C + {}^{18}I - {}^{18}E \tag{Eq. 7}$$

where ^nO_t and $^nO_{t-1}$ are total amount of oxygen isotope n in the water column from the surface to the bottom of lake at the time slice t and t-1 (a step before time t), respectively; ^nP, ^nC, ^nI and ^nE are GP, consumption rate for entire water column, influx from the atmosphere and efflux to the atmosphere, respectively for oxygen isotope n. Eq. 5 can be substituted by column inventory or rates of total dissolved oxygen (Eq. 8).

$$O_t - O_{t-1} = P - C + I - E \tag{Eq. 8}$$

Eq. 6 and Eq. 7 can be obtained by multiplying isotopic composition $(1 + \delta^nO)$ and/or isotope fractionation factor $(1 + {}^n\varepsilon)$ in the Eq. 8.

While a non-steady state model is beyond the scope of this paper, the column inventory approach enables us to introduce dynamics into the calculations of GP and evaluate the feasibility of the mixed layer (ML) approach for estimating PP rates in the Feitsui Reservoir. Because the purpose of this model is to compare two different approaches, rather than produce accurate estimates, and for simplicity, we calculated the GP rates using Eq. 2 and present the ML approach GP rates to column inventory (CI) approach GP rates ratio (Fig. 7). Overall, the GP rates obtained from the ML and CI model showed a good agreement with each other, indicating the calculation of GP rates using a mixed layer model may be valid for the Feitsui Reservoir, not only for open oceans. A better fit between the respective rates may be obtained using lambda slope

0.520, although the reasons for this remain presently unclear. Further adjustments of $^{17}\Delta_{eq}$ and $^{17}\Delta_{bio}$ could also improve the fit.

4.4 Comparisons between $^{17}\Delta$ GP and ^{14}C GP rates

While both methods aim to evaluate the natural GP rates, direct comparisons between estimates from the 'dual delta' method and from the ^{14}C bottle incubation are impractical because of the principal differences in the methodologies (in situ vs. in vitro). Each method provides rates integrated over different spatial and temporal scales, and clearly methodological biases are associated with each. A number of studies have addressed the 'dual delta' GP/^{14}C-GP in the ocean, but the ratios were found to vary significantly from 2.2 (Quay et al. 2010) to 8.2±4.0 (Stanley et al. 2010; see also Juranek and Quay 2013 for an extensive review). The variability in the ratios remains a conundrum. Overall, the 'dual delta' GP method showed a tendency to yield higher production rates. The factors responsible for the variability in the GP/^{14}C-GP have however yet to be properly identified, before the gross O$_2$ production and carbon fixation can be properly linked and compared.

Contrasting the GP rates from 'dual delta' approach and the ^{14}C-GP rates (Table 2 and Fig. 6) we note that both estimates show a very similar trend. Moreover the production rates are on the same order of magnitude, with the average GP/^{14}C-GP ratio of 0.6±0.3. Although, due to the reasons mentioned above, it is unclear why the respective GP rates may agree or disagree, our results support the findings from an earlier study by Luz and Barkan (2000) who demonstrated near equivalence of gross production rates obtained from incubation-dependent and incubation-independent methods from Lake Kinneret. Presumably, near 1 GP/^{14}C-GP ratios are characteristic of systems with shallow mixed-layer and rapid O$_2$ turnover, such as subtropical reservoirs in general, including the Feitsui Reservoir. Moreover, our results showed less variation in the overall GP rates throughout the year and generally lower values than ^{14}C-GP which could be attributed to the integration on which each method operates. The disparity between the $^{17}\Delta$ GP and ^{14}C GP rates from AUG14 and early SEP14 could be explained by the shallow summer mixed layer, which would provide minimal GP rates due to the limitations of this approach. Conversely, it could also be that the ^{14}C-GP is overestimating the production rates particularly during this period, when algal blooms are more likely to occur. This highlights one of the key assets of the GP method, which in principle is not significantly affected by small-scale short-term events. Onwards DEC14 the 'dual delta' GP rates and ^{14}C-GP show a close fit.

4.5 Typhoon effects

Passing of tropical cyclones had been documented to cause entrainment and upwelling or 'atmospheric pumping,' injecting nutrients into the mixed layer which may significantly elevate PP. In the South China Sea, Lin et al. (2003) reported that the occurrence of only a moderate cyclone led to a 30-fold increase in the concentration of surface Chl *a*. Ko et al. (2015)

17

studied the phytoplankton responses to typhoons in the Feitsui Reservoir and found a twofold increase in the phytoplankton level during typhoon periods. While in regions with deep mixed layer and nutricline, typhoon events may not be sufficient to increase PP or induce phytoplankton blooms (Lin 2012). The effect of typhoon events on ecosystems is however complex and difficult to document properly because of their sporadic occurrence. Although our data are too limited to draw solid conclusions, we briefly discuss our results in context of typhoon events.

Two typhoons closely affected the north-eastern Taiwan and the Feitsui Reservoir during our study period. Typhoon Fung Wong hit Taiwan on the 22nd of September 2014 and typhoon Chan Hom on the 10th of July 2015, 1 and 4 days before the sample collection, respectively. Post-typhoon sampling occasions are indicated in Table 2. On both occasions, we found a considerable increase in the GP in the mixed layer (to 912 and 1195 mg C m^{-2} d^{-1}), representing approximately a 3-fold increase in the GP rates obtained otherwise (Fig. 6). This corresponds to 13 and 33 per meg increase in surface $^{17}\Delta$. However, short episodic events of high production are normally expected to average out by the lower background $^{17}\Delta$ of the mixed layer due to elevated gas exchange with air. It is plausible that if the mixed layer is very shallow and the photosynthetic O_2 production is high, the elevated $^{17}\Delta$ signal would remain for an extended period of time. Alternatively, increased $^{17}\Delta$ values could arise from ventilation from water below the mixed layer or enhanced vertical mixing. Greater K caused by higher wind speeds during a typhoon event could explain the higher GP rates; however, it does not explain the increase in $^{17}\Delta$ signal. Nevertheless it is important to note that these GP rates should be considered as minimum values, because on both occasions the thermocline was situated in the photic zone and therefore some of the production also took place below the mixed layer.

5 Conclusions

In summary, the $^{17}\Delta$ and $\Delta O_2/Ar$ values showed strong seasonal and vertical variations, enabling us to monitor the photosynthetic activity versus atmospheric O_2 input in a freshwater system. The 'dual delta' GP and ^{14}C-GP estimates were consistent on the same order of magnitude with the GP/^{14}C-GP ratio of 0.6±0.3 throughout the study. Although the interpretation of the results is not straightforward, the combined $^{17}\Delta$ and $\Delta O_2/Ar$ tracer offers us a new perspective on studying primary production rates in situ. We encourage the use of this technique to evaluate and improve our understanding of the carbon cycling. Further comparisons between the $^{17}\Delta$ and ^{14}C bottle incubation and any other approach, are needed on various spatial and temporal scales and in particular in dynamic and well-characterised environments that could serve as 'natural laboratories', such as the Feitsui Reservoir.

Acknowledgements

18

References

Abe O. and Yoshida N. 2003. Partial pressure dependency of $^{17}O/^{16}O$ and $^{18}O/^{16}O$ of molecular oxygen in the mass spectrometer. Rapid Commun Mass Spectrom 17(5): 395-400.

Barkan, E., Luz, B., 2003. High-precision measurements of $^{17}O/^{16}O$ and $^{18}O/^{16}O$ of O_2 and O_2/Ar ratio in air. Rapid Commun

10   Mass Spectrom 17, 2809-2814.

Barkan, E., Luz, B., 2005. High-precision measurements of $^{17}O/^{16}O$ and $^{18}O/^{16}O$ ratios in H_2O. Rapid Commun Mass Spectrom 19:3737-3742.

Benson B.B., Krause Jr., D.K., 1984. The concentration and isotopic fractionation of oxygen dissolved in freshwater and seawater in equilibrium with the atmosphere. Limnol. Oceanogr. 29(3): 620-632.

15 Craig H. and Hayward T. 1987. Oxygen Supersaturation in the Ocean: Biological Versus Physical Contributions. Science 235(4785): 199-202. doi: 10.1126/science.235.4785.199

Castro-Morales, K., Cassar, N., Shoosmith, D.R., Kaiser, J., 2013. Biological production in the Bellingshausen Sea from oxygen-to-argon ratios and oxygen triple isotopes. Biogeosciences 10, 2273-2291.

Cole, J.J., Prairie, Y.T., Caraco, N.F., McDowell, W.H., Tranvik, L.J., Striegl, R.G., Duarte, C.M., Kortelainen, P.,

20   Downing, J.A., Middelburg, J.J., Melack, J., 2007. Plumbing the Global Carbon Cycle: Integrating Inland Waters into the Terrestrial Carbon Budget. Ecosystems 10, 172-185.

Clark, J.F., Schlosser, P., Simpson, H.J., Stute, M., Wanninkhof, R., Ho, D.T., 1995. Relationship between Gas Transfer Velocities and Wind Speeds in The Tidal Hudson River Determined by the Dual Tracer Technique. In B. J ̈ahne and E. Monahan (eds.), Air-Water Gas Transfer. AEON Verlag.

25 Crusius, J., Wanninkhof, R., 2003. Gas exchange at low wind speeds over a lake. Limnology and Oceanography 48, 1010-1017 .

Dean, W. and Gorham, E., 1998. Magnitude and significance of carbon burial in lakes, reservoirs, and peatlands. Geology, 26(6): 535-538.

Emerson, S., Quay, P.D., Stump, C., Wilbur, D., Schudlich, R., 1995. Chemical tracers of productivity and respiration in the

30   subtropical Pacific Ocean. Journal of Geophysical Research 100, 15873.

Emerson, S., P. Quay, D. Karl, C. Winn, L. Tupas, and M. Landry, 1997. Experimental determination of the organic carbon flux from open-ocean surface waters, Nature, 389, 951–954.

Hamme, R.C., Cassar, N., Lance, V.P., Vaillancourt, R.D., Bender, M.L., Strutton, P.G., Moore, T.S., DeGrandpre, M.D., Sabine, C.L., Ho, D.T., Hargreaves, B.R., 2012. Dissolved O_2/Ar and other methods reveal rapid changes in productivity during a Lagrangian experiment in the Southern Ocean. Journal of Geophysical Research 117, C00F12.

Harrison W.G. and Harris L.R., 1986. Isotope-dilution and its effects on measurements of nitrogen and phosphorous uptake by oceanic microplankton. Mar. Ecol. Prog. Ser. 27: 253-261.

Hendricks, M.B., Bender, M.L., Barnett, B.A., 2004. Net and gross O_2 production in the southern ocean from measurements of biological O_2 saturation and its triple isotope composition. Deep Sea Research Part I: Oceanographic Research Papers 51, 1541-1561.

Hendricks, M.B., Bender, M.L., Barnett, B.A., Strutton, P., Chavez, F.P., 2005. Triple oxygen isotope composition of dissolved O_2 in the equatorial Pacific: A tracer of mixing, production, and respiration. Journal of Geophysical Research 110, C12021, doi:10.1029/2004JC002735

Ho, D.T., Law, C.S., Smith, M.J., Schlosser, P., Harvey, M., Hill, P., 2006. Measurements of air-sea gas exchange at high wind speeds in the Southern Ocean: Implications for global parameterizations. Geophysical Research Letters 33.

Itoh, M., Kobayashi, Y., Chen, T.Y., Tokida, T., Fukui, M., Kojima, H., Miki, T., Tayasu, I., Shiah, F.-K., and Okuda, N., 2015. Effect of inter-annual variation in winter vertical mixing on CH4 dynamics in a subtropical reservoir. J. Geophys. Res. – Biogeosciences, 120 (7): 1177–1195.

Jassby, A.D. and Platt, T., 1976. Mathematical formulation of the relationship between photosynthesis and light for phytoplankton. Limnol. Oceanogr., 21: 540-547.

Juranek, L.W., Quay, P.D., 2010. Basin-wide photosynthetic production rates in the subtropical and tropical Pacific Ocean determined from dissolved oxygen isotope ratio measurements. Global Biogeochemical Cycles, 24, GB2006, doi:10.1029/2009GB003492.

Juranek, L.W., Quay, P.D., 2013. Using triple isotopes of dissolved oxygen to evaluate global marine productivity. Ann Rev Mar Sci 5, 503-524.

Juranek, L.W., Quay, P.D., Feely, R.A., Lockwood, D., Karl, D.M., Church, M.J., 2012. Biological production in the NE Pacific and its influence on air-sea CO_2 flux: Evidence from dissolved oxygen isotopes and O_2 /Ar. Journal of Geophysical Research 117 .

Keedakkadan, H.R. and Abe, O., 2015. Cryogeni separation of an oxygen-argon mixture in natural air samples for the determinationof isotope and molecular ratios. Rapid Commun. Mass Spectrom. 29(8): 775-781.

Krause Jr., D.K., Benson B.B., 1989.The solubility and Isotopic Fractionation of Gases in Dilute Aqueous Solution. IIa. Solubilities of the Noble Gases. Journal of Solution Chemistry, 18(9).

Ko, C.-Y., Lai, C.-C., Chen, T.-Y., Hsu, H.-H., Shiah, F.-K. (2015) Typhoon effects on phytoplankton responses in a semi-closed freshwater ecosystem. Marine and Freshwater Research, http://dx.doi.org/10.1071/MF14294

Kuo, J.-T., Wen-Cheng Liu, Ruey-Tyng Lin, Wu-Seng Lung, Ming-Der Yang, Chou-Ping Yang, and Show-Chyuan Chu, 2003. Water quality modeling for the Feitsui Reservoir in northern Taiwan. Journal of the American Water Resource Association 39(4): 671-687.

Kuo, J.T., Wang, Y.Y., Lung, W.S., 2006. A hybrid neural-genetic algorithm for reservoir water quality management. Water Res 40: 1367-1376.

Laskar A. H., Huang J.-C., Hsu S.-C., Bhattacharya S. K., Wang C.-H. and Liang M.-C. 2014. Stable isotopic composition of near surface atmospheric water vapour and rain-vapour interaction in Taipei, Taiwan. Journal of Hydrology 519: 2091-2100.

Laws, E.A., 1991. Photosynthetic quotients, new production and net community production in the open ocean. Deep-Sea Research I 38 (1), 143–167.

Laws, E.A., Landry, M.R., Barber, R.T., Campbell, L., Dickson, M.L., Marra, J., 2000. Carbon cycling in primary production bottle incubations: inferences from grazing experiments and photosynthetic studies using C-14 and O-18 in the Arabian Sea. Deep-Sea Research II 47 (7–8), 1339–1352.

Lewis, W., 2011. Global primary production of lakes: 19th Baldi Memorial Lecture. Inland Waters 1, 1-28.

Lin, I.-I., Liu, W.-T., Wu, C.-C., Wong, G.T.F., Hu, C., Chen, Z., Liang, W.-D., Yang, Y. and Liu, K.-K. 2003. New evidence for enhanced ocean primary production triggered by tropical cyclone. Geophysical Research Letters 30(13).

Lin, I.-I. 2012, Typhoon-induced phytoplankton blooms and primary productivity increase in the western North Pacific subtropical ocean. Journal of Geophysical Research, 117: C03039.

Luz, B., Barkan, E., Bender, M.L., Thiemens, M.H., Boering, K.A., 1999. Triple-isotope composition of atmospheric oxygen as a tracer of biosphere productivity. Nature, 400.

Luz B. and Barkan E. 2000. Assessment of Oceanic Productivity with the Triple-Isotope Composition of Dissolved Oxygen. Science 288: 2028-2031.

Luz, B., Barkan, E., Sagi, Y., Yacobi, Y.Z., 2002. Evaluation of community respiratory mechanisms with oxygen isotopes: A case study in Lake Kinneret. Limnology and Oceanography 47, 33-42.

Luz, B. and Barkan, E., 2005. The isotopic ratios $^{17}O/^{16}O$ and $^{18}O/_{16}O$ in molecular oxygen and their significance in biogeochemistry. Geochimica et Cosmochimica Acta 69, 1099-1110.

Luz, B. and Barkan, E., 2009. Net and gross oxygen production from O_2 /Ar, $^{17}O/^{16}O$ and $^{18}O/^{16}O$ ratios. Aquatic Microbial Ecology 56, 133-145.

Mahata, S., Bhattacharya, S. K., Wang, C.-H., Liang, M.-C., 2013. Oxygen isotope exchange between O_2 and CO_2 over hot platinum: an innovative technique for measuring $\Delta^{17}O$ in CO_2, Analytical Chemistry, 85(14), 6894-6901.

21

Mahata, S., Bhattacharya, S. K., Liang, M.-C., 2016. An improved method of high precision determination for $\Delta^{17}O$ of CO_2 by catalyzed exchange with O_2 using hot platinum, Rapid Communications in Mass Spectrometry, 30, 119-131, DOI:10.1002/rcm.7423.

Marra J. (2002) Approaches to the measurement of plankton production. Phytoplankton productivity: carbon assimilation in marine and freshwater ecosystem. P. J. leB. Willams, D.N. Thomas, C.S. Reynolds. Cambridge, Blackwells, 78-108.

Munro, D. R., Quay P.D., Juranek L. W., and Goericke R., 2013. Biological production rates off the Southern California coast estimated from triple O_2 isotopes and O_2 : Ar gas ratios, Limnol. Oceanogr., 58(4): 1312–1328, doi:10.4319/lo.2013.58.4.1312.

Pai, S.C., Gong, G.C., and Liu, K.K., 1993. Determination of dissolved oxygen in seawater by direct spectrophotometry of total iodine. Marine Chemistry 41:343-351.

Prokopenko, M.G., Pauluis, O.M., Granger, J., Yeung, L.Y., 2011. Exact evaluation of gross photosynthetic production from the oxygen triple-isotope composition of O_2: Implications for the net-to-gross primary production ratios. Geophysical Research Letters 38, L14603.

Quay, P.D., Peacock, C., Björkman, K., Karl, D.M., 2010. Measuring primary production rates in the ocean: Enigmatic results between incubation and non-incubation methods at Station ALOHA. Global Biogeochemical Cycles, 24, GB3014, doi:10.1029/2009GB003665.

Quay, P., J. Stutsman, and T. Steinhoff, 2012. Primary production and carbon export rates across the subpolar N. Atlantic Ocean basin based on triple oxygen isotope and dissolved O_2 and Ar gas measurements, Global Biogeochem. Cycles, 26, GB2003, doi:10.1029/2010GB004003.

Reuer, M. K., Barnett B. A., Bender M. L, Falkowski P. G. and Hendricks M. B., 2007. New estimates of Southern Ocean biological production rates from O_2/Ar ratios and the triple isotope composition of O_2, Deep Sea Res., Part I, 54(6), 951–974, doi:10.1016/j.dsr.2007.02.007.

Sarma, V.V.S.S., Abe, O., Hashimoto, S., Hinuma, A., Saino, T., 2005. Seasonal variations in triple oxygen isotopes and gross oxygen production in the Sagami Bay, central Japan. Limnology and Oceanography 50: 544-552.

Sarma, V.V.S.S., Abe, O., Hinuma, A., Saino T., 2006. Short-term variation of triple oxygen isotopes and gross oxygen production in the Sagami Bay, central Japan. Limnol. Oceanogr. 51(3): 1432-1442.

Sarma, V.V.S.S., Abe, O., Saino, T., 2008. Spatial variations in time-integrated plankton metabolic rates in Sagami Bay using triple oxygen isotopes and O_2:Ar ratios. Limnol. Oceanogr. 53(5): 1776-1783.

Schlitzer R. 2015. Ocean Data View, odv.awi.de.

Spitzer W.S. and Jenkins W.J., 1989. Rates of vertical mixing, gas exchange and new production-estimates from seasonal gas cycles in the upper ocean near Bermuda. J Mar Res 47(1):169-196.

22

Shiah, F.-K., Gong, G.-C., Liu, K.-K., 1996. Light effects on phytoplankton photosynthetic performance in the southern East China Sea north of Taiwan. Bot. Bull. Acad. Sin. 37: 133-140.

Shiau, J.-T., Wu, F.-C., 2010. A dual active-restrictive approach to incorporating environmental flow targets into existing reservoir operation rules. Water Resources Research 46.

Stanley, R.H.R., Kirkpatrick, J.B., Cassar, N., Barnett, B.A., Bender, M.L., 2010. Net community production and gross primary production rates in the western equatorial Pacific. Global Biogeochemical Cycles, 24, GB4001, doi:10.1029/2009GB003651.

Steeman-Nielsen, E. 1952. The use of radioactive carbon (^{14}C) for measuring organic production in the sea. Journal du Conseil, 18: 117 -140.

Tranvik, L.J., Downing, J.A., Cotner, J.B., Loiselle, S.A., Striegl, R. G., Ballatore, T.J., Dillon, P., Finlay K., Fortino, K., 2009. Lakes and reservoirs as regulators of carbon cycling and climate. Limnol. Oceanogr. 54(6, part 2): 2298-2314.

Tseng, Y.-F., Hsu, T.-C., Chen, Y.-L., Kao, S.-J., Wu, J.-T., Lu, J.-C., Lai, C.-C., Kuo, H.-Y., Lin, C.-H., Yamamoto, Y., Xiao, T., Shiah, F.-K. 2010. Typhoon effects on DOC dynamics in a phosphate-limited reservoir. Aquatic Microbial Ecology, 60: 247-260.

Vachon, D., Prairie, Y.T., 2013. The ecosystem size and shape dependence of gas transfer velocity versus wind speed relationships in lakes. Canadian Journal of Fisheries and Aquatic Sciences 70: 1757-1764.

Valdespino-Castillo P.M., Merino-Ibarra M., Jimenez-Contreras J., Castillo-Sandoval F.S.,Ramirez-Zierold J.A. 2014. Community metabolism in a deep (stratified) tropical reservoir during a period of high-water fluctuations. Environ. Monit. Assess. 186: 6505-6520.

Wanninkhof, R., 1992. Relationship between wind speed and gas exchange over the ocean. Journal of Geophysical Research 97, 7373.

Wanninkhof, R., Ledwell, J.R., Broecker, W.S., Hamilton, M., 1987. Gas exchange on Mono Lake and Crowley Lake, California. Journal of Geophysical Research 92, 14567.

Wanninkhof, R., Asher, W.E., Ho, D.T., Sweeney, C., McGillis, W.R., 2009. Advances in quantifying air-sea gas exchange and environmental forcing. Ann. Rev. Mar. Sci. 1: 213-244.
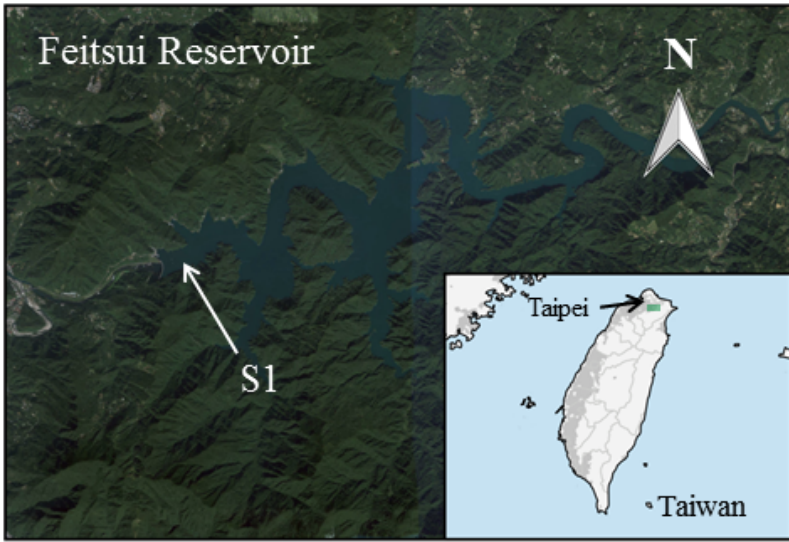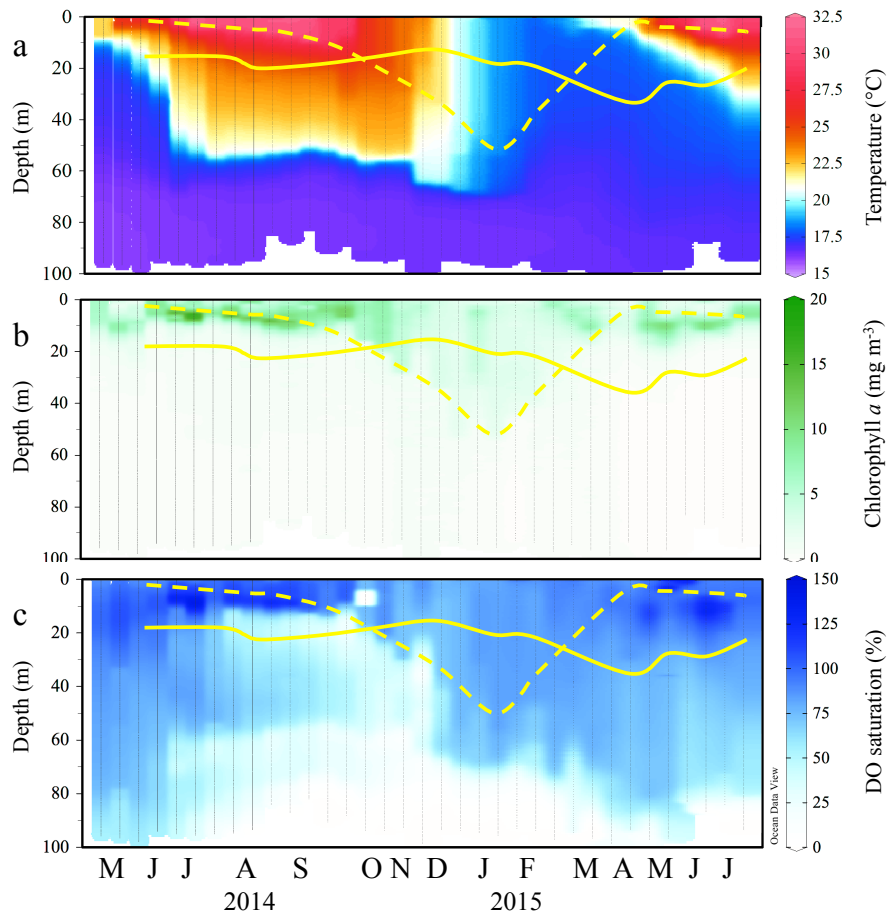
23

Figure 1. Location of Feitsui Reservoir northern Taiwan. Small green rectangle indicates the enlarged satellite map of the reservoir with the position of the long-term station S1 near the dam indicated.

Figure 2. Annual variability in a) temperature (°C), b) chlorophyll a concentration (mg m^{-3}), and c) dissolved oxygen saturation (%) from S1 in the Feitsui Reservoir (S1). Profile data normally collected on weekly basis throughout the warmer months and every two weeks in winter. Solid yellow line indicates the limit of euphotic zone and dashed yellow line the depth of mixed layer.
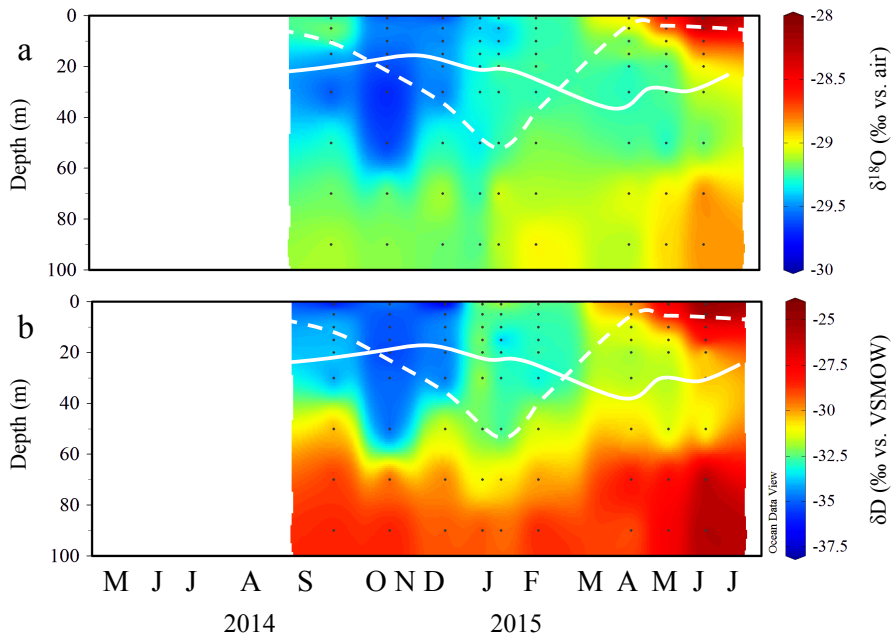
25

Figure 3. Annual variability in a) δ¹⁸O of water O₂ (‰, vs. VSMOW), and b) δᴰ (‰, vs. VSMOW). Solid white line indicates the limit of euphotic zone and dashed white line the depth of mixed layer.
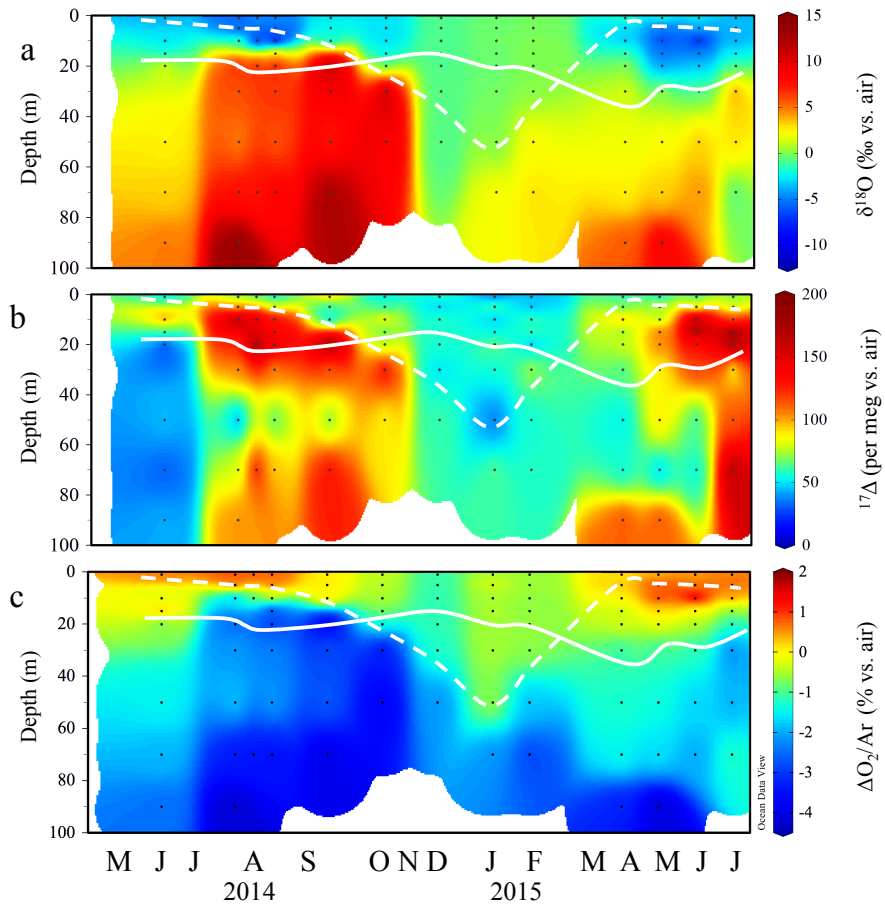
Figure 4. Annual variability in a) $\delta^{18}O$ of dissolved O_2 (‰, vs. air), b) $^{17}\Delta$ (per meg, vs. air) and c) $\delta O_2/Ar$ (‰, vs. air) in Feitsui Reservoir. Solid white line indicates the limit of euphotic zone and dashed white line shows the depth of mixed layer.
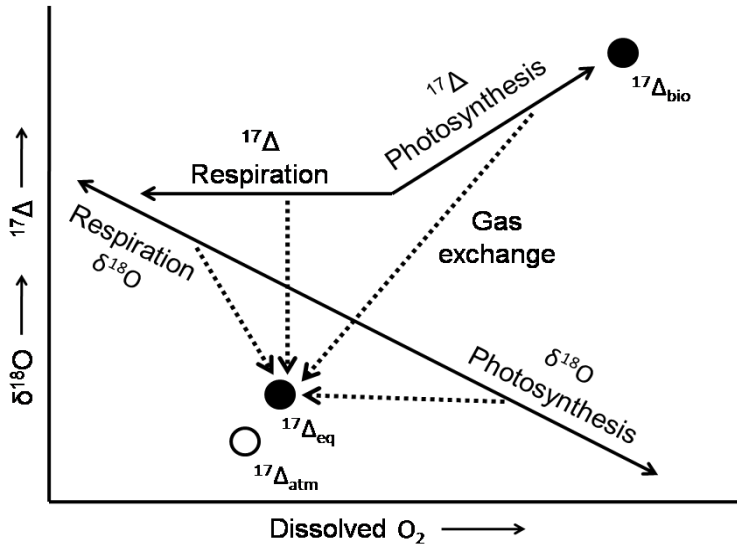
Figure 5. A schematic diagram showing the effects of photosynthesis, respiration and air-water gas exchange on dissolved O_2 concentrations, $\delta^{18}O$ and $^{17}\Delta$. $\delta^{18}O$ changes with all the processes and additionally is also affected by mixing. Because of non-mass dependent processes occurring in the stratosphere, the $^{17}\Delta$ of O_2 in air has a different signal to the O_2 produced biologically where
5 **fractionation is mass-dependent. $^{17}\Delta$ increases due to photosynthesis, decreases due to gas exchange but is not affected by respiration. Respiration removes O_2 and decreases the dissolved O_2 concentration but fractionates O_2 isotopes in a mass-dependent way, which does not affect the relative proportion of $\delta^{17}O$ and $\delta^{18}O$ and therefore the $^{17}\Delta$. $^{17}\Delta_{bio}$ is the maximum value of pure biological signal, which amounts to $^{17}\Delta$ of water. The slope of $^{17}\Delta$ increase towards $^{17}\Delta_{bio}$ is the kinetic slope λ for respiration ($\lambda =$ 0.518). $^{17}\Delta_{eq}$ is the O_2 at air-water equilibrium, which has a small offset from $^{17}\Delta_{atm}$, which is by definition 0, due to fractionation at**
10 **equilibrium where $\delta^{17}O$ and $\delta^{18}O$ slopes during invasion and evasion follow a slightly different slope to that of respiration.**
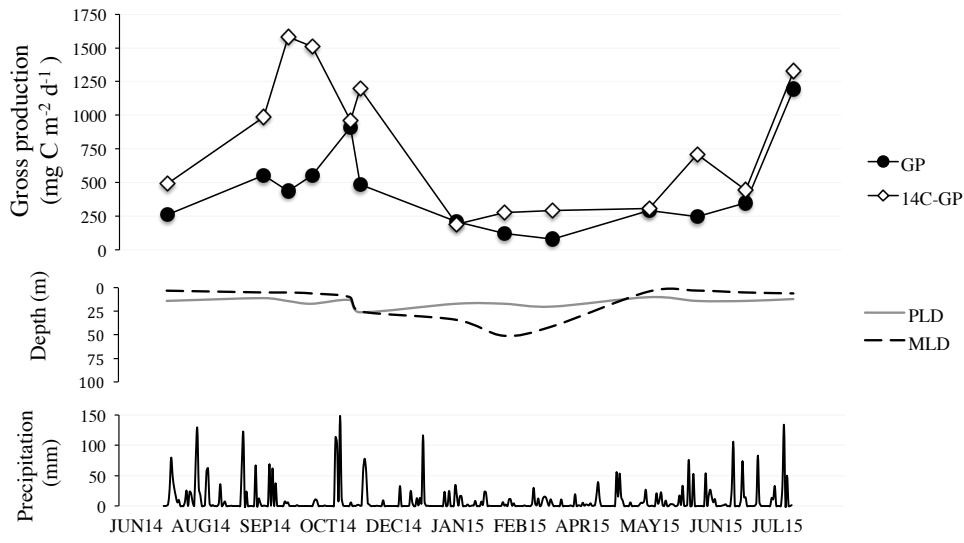
28

Figure 6. Comparison between 'dual-delta' GP estimates and ^{14}C-GP rates. PLD and MLD indicate photosynthetic layer depth and mixed layer depth, respectively and precipitation shows the total daily rainfall.
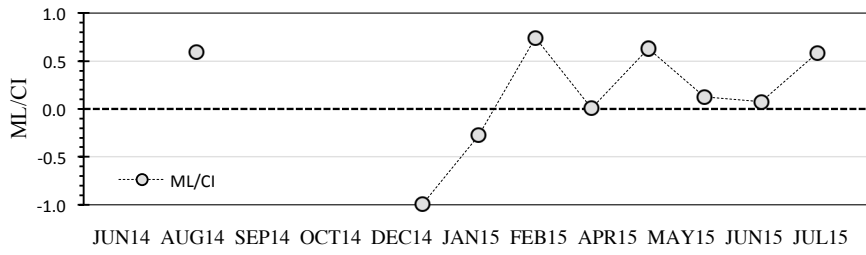
29

Figure 7. Comparison between production rates obtained from mixed layer model (ML, Luz and Barkan 2000) and oure whole column inventory approach (CI).

Table 1. Air-equilibrated water results.

Deionised water sample	$\delta O_2/Ar$ (‰) vs. air	$\Delta O_2/Ar$ (%) vs. air	$\delta^{17}O$ (‰) vs. air	$\delta^{18}O$ (‰) vs. air	$^{17}\Delta$[a] (per meg) vs. air
1	216	0	0.346	0.645	10
2	226	0	0.314	0.591	6
3	226	0	0.310	0.573	11

[a] Corrected for Ar interference

5

Table 2. Summary of mixed layer PP rates in the Feitsui Reservoir from June 2014 to July 2015. Dates marked with an asterisk indicate post-typhoon sampling days. GP, NP and ^{14}C-GP are in mg C m^{-2} d^{-1}.

Date	Abbrev.	PLD[a] (m)	MLD[b] (m)	C_o (mmol m^{-3})	K from U (m day^{-1})	$\Delta O_2/Ar$ (%) vs. air	GP[c]	NP	NP/ GP	^{14}C-GP
10/06/2014	JUN14	14	3	249.01	0.21	0.6	262	680	2.6	492
19/08/2014	AUG14	11	5	232.20	0.27	0.8	552	1214	2.2	988
26/08/2014	AUG14	14	5	232.20	0.30	0.7	436	1191	2.7	1580
02/09/2014	SEP14	17	6	232.20	0.35	0.7	554	1347	2.4	1510
23/09/2014*	SEP14	13	10	240.36	1.15	0.1	912	524	0.6	961
28/10/2014	OCT14	26	25	258.23	0.56	-0.7	486	-2168	-4.5	1197
09/12/2014	DEC14	17	34	273.24	0.64	-1.1	207	-4556	-22.0	190
20/01/2015	JAN15	17	51	289.89	0.65	-0.5	121	-2008	-16.6	275
10/02/2014	FEB15	20	41	295.85	0.69	-0.6	79	-2811	-35.6	292
14/04/2015	APR15	10	4	278.59	0.48	0.1	293	360	1.2	307
19/05/2015	MAY15	14	3	244.62	0.40	0.3	247	764	3.1	708
23/06/2015	JUN15	14	5	232.20	0.36	0.5	348	1018	2.9	442
14/07/2015*	JUL15	12	6	240.36	1.00	0.6	1195	3491	2.9	1328

[a] Photic layer depth
[b] Mixed layer depth
[c] Following Prokopenko et al. (2011) and Kaiser (2011)

32